Forest Ecology and Management 366 (2016) 193–207

Contents lists available at ScienceDirect

Forest Ecology and Management

journal homepage: www.elsevier.com/locate/foreco

Complex mountain terrain and disturbance history drive variation in forest aboveground live carbon density in the western Oregon Cascades, USA

Harold S.J. Zald [a,*], Thomas A. Spies [b], Rupert Seidl [c], Robert J. Pabst [a], Keith A. Olsen [a], E. Ashley Steel [d]

[a] Oregon State University, College of Forestry, Corvallis, OR 97331, USA
[b] USDA Forest Service, Pacific Northwest Research Station, Corvallis, OR 97331, USA
[c] University of Natural Resources and Life Sciences (BOKU), Institute of Silviculture, Vienna, Austria
[d] USDA Forest Service, Pacific Northwest Research Station, Seattle, WA 98103, USA

ARTICLE INFO

Article history:
Received 4 September 2015
Received in revised form 27 January 2016
Accepted 31 January 2016
Available online 19 February 2016

Keywords:
Forest carbon
Lidar
Topography
Forest management
Wildfire
Landscape heterogeneity

ABSTRACT

Forest carbon (C) density varies tremendously across space due to the inherent heterogeneity of forest ecosystems. Variation of forest C density is especially pronounced in mountainous terrain, where environmental gradients are compressed and vary at multiple spatial scales. Additionally, the influence of environmental gradients may vary with forest age and developmental stage, an important consideration as forest landscapes often have a diversity of stand ages from past management and other disturbance agents. Quantifying forest C density and its underlying environmental determinants in mountain terrain has remained challenging because many available data sources lack the spatial grain and ecological resolution needed at both stand and landscape scales. The objective of this study was to determine if environmental factors influencing aboveground live carbon (ALC) density differed between young versus old forests. We integrated aerial light detection and ranging (lidar) data with 702 field plots to map forest ALC density at a grain of 25 m across the H.J. Andrews Experimental Forest, a 6369 ha watershed in the Cascade Mountains of Oregon, USA. We used linear regressions, random forest ensemble learning (RF) and sequential autoregressive modeling (SAR) to reveal how mapped forest ALC density was related to climate, topography, soils, and past disturbance history (timber harvesting and wildfires). ALC increased with stand age in young managed forests, with much greater variation of ALC in relation to years since wildfire in old unmanaged forests. Timber harvesting was the most important driver of ALC across the entire watershed, despite occurring on only 23% of the landscape. More variation in forest ALC density was explained in models of young managed forests than in models of old unmanaged forests. Besides stand age, ALC density in young managed forests was driven by factors influencing site productivity, whereas variation in ALC density in old unmanaged forests was also affected by finer scale topographic conditions associated with sheltered sites. Past wildfires only had a small influence on current ALC density, which may be a result of long times since fire and/or prevalence of non-stand replacing fire. Our results indicate that forest ALC density depends on a suite of multi-scale environmental drivers mediated by complex mountain topography, and that these relationships are dependent on stand age. The high and context-dependent spatial variability of forest ALC density has implications for quantifying forest carbon stores, establishing upper bounds of potential carbon sequestration, and scaling field data to landscape and regional scales.

1. Introduction

Forests play a critical role as a carbon (C) sink of atmospheric CO_2, partially offsetting anthropogenic greenhouse gas emissions and thereby mitigating their effect on climate change (Goodale et al., 2002; Woodbury et al., 2007; Pan et al., 2011). Forest C density (C stored per unit land area) varies tremendously at stand, regional, and global spatial scales (Smithwick et al., 2002;

* Corresponding author.
E-mail addresses: harold.zald@oregonstate.edu (H.S.J. Zald), tom.spies@oregonstate.edu (T.A. Spies), rupert.seidl@boku.ac.at (R. Seidl), rob.pabst@oregonstate.edu (R.J. Pabst), keith.olsen@oregonstate.edu (K.A. Olsen), asteel@fs.fed.us (E.A. Steel).

http://dx.doi.org/10.1016/j.foreco.2016.01.036
0378-1127/

Bradford et al., 2010; Pan et al., 2011; Gray and Whittier, 2014). Given the importance of forests in the global C cycle, understanding the patterns and sources of variability of forest C density across scales is critical for inventory and monitoring of forest C in support of ecosystem management for climate change mitigation. For example, estimates of forest C pools and fluxes are one component of national and international reporting obligations on greenhouse gas emissions (UNFCCC, 2009; US EPA, 2015). Furthermore, quantifying the patterns and sources of variability of forest C is important for parameterization of simulation models used to understand how different management strategies, disturbance agents, and climate change may influence forest C sequestration and emissions (Kindermann et al., 2013; Seidl et al., 2014a,b).

Many factors are known to influence forest C density, including climate (Chen et al., 2003; Baccini et al., 2004), soil conditions (Oren et al., 2001), forest age (Pregitzer and Euskirchen, 2004), disturbance history and land management (Houghton et al., 1999; Goodale et al., 2002; Kashian et al., 2006; Kurz et al., 2008), species diversity (Bunker et al., 2005; Bradford, 2011), and vegetation structural complexity (Hardiman et al., 2011; Fahey et al., 2015). Variation of forest C density may be especially pronounced in mountainous regions, which contain approximately one quarter of the world's forests (FAO, 2011). Steep gradients of elevation and physiography that characterize mountainous terrain strongly influence climate (Daly et al., 1994, 2010; Lundquist and Cayan, 2007; Dobrowski et al., 2009), soil characteristics (Tromp-van Meerveld and McDonnell, 2006; Griffiths et al., 2009; Pelletier and Rasmussen, 2009), and disturbance regimes (Heyerdahl et al., 2001; Taylor and Skinner, 2003). Furthermore, in complex mountainous terrain individual environmental factors often have interactive, hierarchical, and multi-scale relationships with forest composition and structure (Urban et al., 2000; Seidl et al., 2012).

Estimates of forest C storage and its variability are often made at regional to global scales (Smithwick et al., 2002; Hudiburg et al., 2009; Pan et al., 2011). There is a rich history of ecological research investigating landscape and regional environmental controls on forest productivity and biomass in mountains (Assmann and Franz, 1963; Whittaker, 1966; Whittaker et al., 1974; Whittaker and Niering, 1975; Bormann and Likens, 2012; Nabuurs et al., 2008; Pretzsch et al., 2014). However, we still lack a understanding of the relative importance of environmental factors driving forest C density in mountain forest landscapes that are a mixture of managed and unmanaged stands (although see Baraloto et al., 2011; Seidl et al., 2012). Often, quantification of forest C and its environmental controls has been focused on the importance of old-growth forests and the upper bounds of forest C (Smithwick et al., 2002; Hudiburg et al., 2009). Younger managed forests have received less attention, in part due to their lower C stores, yet they can occupy large areas and are the location of much of the potential future additions to C stores in most landscapes. Furthermore, conservation of old-growth forests suggests future management activities will be increasingly concentrated in younger forests. Relatively few studies have compared environmental influences on forest C between young and old forests (although see Berenguer et al., 2014). The lack of knowledge as to how environmental factors drive forest C density in old versus young forests limits development of forest carbon management strategies and limits our ability to scale up results for landscapes that are a mosaic of managed and unmanaged forests.

This knowledge gap may in part be due to methodological limitations of measuring forest C and its spatial variability. Empirical estimates of forest C pools and fluxes are generally made using plot-based measurements (Smithwick et al., 2002), micrometeorological towers (Baldocchi et al., 2001), or optical satellite imagery (Turner et al., 2003). These data types often occur at different spatial and temporal scales, and each have specific limitations for quantifying the fine-grained spatial variability of forest C density and its underlying controls across landscapes. Plot-based measurements of forest C use biometric methods that are accurate, but they are labor intensive and sample intensities in traditional plot-based forest inventories may be inadequate in heterogeneous landscapes (Bradford et al., 2010). Using flux towers to quantity forest C in heterogeneous landscapes is also problematic, because their spatial resolution can extend hundreds or thousands of meters in tall forests (Baldocchi, 1997), and flux towers measure short-term C flux rather than C stores (i.e., the long-term integral of forest C sequestration). Finally, imagery from Landsat and other satellite passive optical sensors have known sensitivity and saturation limitations when estimating C density in forest types with high leaf area indices, high aboveground live biomass, and complex vertical canopy structure (Turner et al., 1999; Lu, 2006; Duncanson et al., 2010). In contrast to passive remote sensing, light detection and ranging (lidar) is well suited to fine-grained quantification of forest C density and its environmental determinants across landscapes. Lidar can characterize vegetation structure and underlying topography at fine resolutions (Lefsky et al., 2002a), and provide highly accurate estimates of aboveground biomass and carbon (Lefsky et al., 2002b; Li et al., 2008; Asner and Mascaro, 2014). In combination with ancillary data sources, lidar can provide novel insights into the spatial variation of forest C and its underlying controls (Asner et al., 2010).

In this study we coupled lidar data with fine-scale forest inventory data to map and analyze aboveground live carbon (ALC) density of the H.J. Andrews Experimental Forest (HJA), a mountainous forested watershed in the western Cascade Mountains of Oregon, USA. The Pacific Northwest Region of North America has some of the highest forest C densities in the world (Smithwick et al., 2002; Keith et al., 2009). We analyzed patterns of mapped ALC density in relation to climate, topography, and disturbance history. Seidl et al. (2012) previously examined the spatial drivers of forest C density in the old-growth portion of the HJA using correlation analyses and a 500 year landscape simulation model experiment that was validated with lidar-derived estimates of forest C density. Their analyses showed that only about 55% of the variation in C stocks could be explained by environmental drivers, and much of the remaining variation in ALC was attributable to differences in forest composition and structure. Yet, the role of management and disturbance history and its potential interaction with environmental drivers of ALC density was left unexplored by this previous analysis. Here, our primary objectives were thus to quantify how environmental factors influence ALC density, and determine if these factors and their relative importance vary between young managed and old unmanaged portions of the landscape. We hypothesize that environmental drivers should explain more variation of ALC in younger forests, because young forests have less accumulated history of mortality from density dependent and density independent processes (e.g., wind, disease, fire) (Franklin et al., 2002), and both their growth rates and structural development are primarily driven by site productivity (Klinka and Carter, 1990; Larson et al., 2008). In contrast, old forests in the region are characterized by centuries of disturbances ranging from individual tree and small-scale gap formation (Spies and Franklin, 1988; Spies et al., 1990) to larger wildfires of variable severity (Teensma, 1987; Morrison and Swanson, 1990; Tepley et al., 2013). Furthermore, older forests are characterized by more complex patterns and processes of stand development, including significant establishment and growth of shade tolerant trees, and changes in canopy structure and development in older trees compared to young forests (Franklin et al., 2002). As a result of these differences in growth and mortality between young and old forests, we hypothesized that drivers of ALC density vary with age.

2. Materials and methods

2.1. Study area

The study was conducted at the H.J. Andrews Experimental Forest (HJA), located at 44.2°N, 122.2°W in the western Oregon Cascades, USA. The study area of 6369 ha includes the entire drainage basin of Lookout Creek, with elevation ranging from 412 to 1617 m. Lower elevations are underlain by volcanic rocks composed of mudflows, ash flows, and stream deposits; middle elevations are underlain by ash and lava flows; upper elevations are comprised of lava flows (Swanson and James, 1975; Swanson and Jones, 2002). Volcanic, glacial, fluvial, and other geomorphic processes have shaped the topography and soils of the HJA. Glacial landforms of U-shaped valleys characterize the southeastern area of the basin, and western portions have steep slopes, narrow ridges, and narrow valley floors resulting from stream erosion and shallow rapid debris flows. Many areas of moderately sloped irregular terrain are the result of deep, slow moving landslides (Swanson and Swanston, 1977; Pyles et al., 1987). Stream valleys range from steep and narrow chutes to wide alluvial benches. Soils are well-drained and derived from volcanic, colluvium, and residual materials. The climate is maritime Mediterranean, with wet mild winters and dry cool summers. Mean monthly temperatures at low elevations range from near 1 °C in January to 18 °C in July and decline with increasing elevation. Precipitation falls primarily from November to March, averaging 2300 mm yr^{-1} at low elevations to over 3550 mm yr^{-1} at higher elevations. At low elevations precipitation is a mix of rain and snow with snowpack rarely lasting more than a couple of weeks. At higher elevations an increasing fraction of precipitation falls as snow, and seasonal snowpack develops above 1000–1200 m.

Low elevation forests are dominated by Douglas-fir (*Pseudotsuga menziesii* (Mirb.) Franco), western hemlock (*Tsuga heterophylla* (Raf.) Sarg.), and western redcedar (*Thuja plicata* Donn ex D. Don). Upper elevation forests are dominated by noble fir (*Abies procera* Rehd.), Pacific silver fir (*Abies amabilis* Dougl. ex Forbes), mountain hemlock (*Tsuga mertensiana* (Bong.) Carr.), Douglas-fir, and western hemlock. Low and middle elevation forests in this area are highly productive, with carbon stores in excess of 600 Mg ha^{-1} (Smithwick et al., 2002). Douglas-fir is the seral dominant species across much of the HJA, typically developing young even-aged stands after stand-replacing disturbances. Stands over 200 years old exhibit old-growth characteristics such as co-dominance of western hemlock in the overstory, multilayered vertical foliage distribution, and high accumulations of down wood (Spies and Franklin, 1988; Spies et al., 1988; Franklin et al., 2002).

Wildfire and timber harvesting have been the primary disturbances in the study area. The oldest stands at the HJA are over 500 years old, having established after high severity wildfire (Teensma, 1987; Tepley et al., 2013). High and mixed severity fires are the most common fire regimes at the HJA, with fire returns intervals of 80–200 years (Teensma, 1987; Morrison and Swanson, 1990; Tepley et al., 2013). Non-stand replacing fires have also been common, resulting in multiple pathways of successional development and highly variable stand structure (Tepley et al., 2013). When the HJA was established as a research forest in 1948, about 65% of the forest area was old-growth, with the remainder largely mature stands that established after wildfires in the mid-1800s to early 1900s. From 1950 to 1995, about 23% (1496 ha) of the HJA was clear cut, and regenerated as plantations of native conifers. No clear cut harvests have occurred within the HJA since the mid-1990s.

2.2. Data sources

2.2.1. Aboveground live carbon (ALC) density from field plots

Field data of tree species, sizes, and abundance were collected on 708 plots between 2006 and 2009. Plots are associated with multiple vegetation studies at the HJA (see Harmon and Munger, 2005), resulting in different plot sizes (between 0.025 and 0.1 ha) and spatial clustering of plots across the study area. We applied two sets of species-specific allometric equations (Means et al., 1994; Jenkins et al., 2004) to calculate two sets of aboveground live biomass values for all individual trees, summed aboveground live biomass to the plot-level, and applied expansion factors to plot-level values to calculate aboveground live biomass per unit area (Mg ha^{-1}). The correlation between plot-level sums of aboveground live biomass calculated with the two different sets of allometric equations were high and linear across the range of values (Pearson correlation coefficient $r = 0.99$), so we averaged the values derived from the two sets of equations for further analysis. Median plot-level aboveground live biomass was 487.23 Mg ha^{-1}, with 5th and 95th percentile values of 93.66 and 1669.03 Mg ha^{-1}, respectively. Plot-level aboveground live biomass values were divided by two to calculate aboveground live carbon density (ALC, Mg ha^{-1}).

2.2.2. Lidar data, lidar-derived vegetation and topographic variables

Airborne discrete return lidar data was collected by Watershed Science, Inc. (Corvallis, Oregon, USA) on August 10–11 in 2008. Lidar was collected from a fixed wing aircraft equipped with Leica ALS50 Phase II laser scanner with a 105 kHz pulse rate, scan angle of ±14° from nadir, and 50% scan swath overlap. Average pulse return density exceeded 9 points/m^2, and root mean squared error between lidar points and 344 real time kinematic GPS survey points was 0.024 m. Using the lidar point cloud and lidar-derived bare earth digital elevation model (DEM), we calculated gridded variables representing vegetation height and vertical variability using the grid metrics function in FUSION/LDV (McGaughey, 2013). Numerous studies in temperate conifer forests of the Pacific Northwest region have consistently found a small number of lidar metrics characterizing vegetation height, canopy cover, and vertical foliage distribution to be effective predictors of forest structure and biomass (Hudak et al., 2008; Li et al., 2008; Kane et al., 2010; Zald et al., 2014). Based on these prior studies, we considered the mean (H_{mean}), variance (H_{var}), and 95th percentile (H_{95}) height of lidar first returns, and vegetation cover as the percentage of all lidar returns >2 m (COV_2) and >40 m (COV_{40}) above ground as potential predictor variables of plot-based ALC. We also considered rumple (canopy surface area/ground surface area, Parker et al., 2004; Kane et al., 2010), and a custom index (INDEX3), which explained additional variability of ALC beyond standard lidar variables. INDEX3 was calculated by computing canopy point density in 1 m vertical bins throughout the range of H_{95} in the study area (1–64 m), multiplying each bin by its height above ground, and summing the binned products. INDEX3 produces higher values for foliage in the upper canopy of trees, accounting for higher biomass in trees with broad upper canopies (and possibly thicker boles) compared to trees with narrow upper canopies of similar height. Rumple and INDEX3 were strongly correlated, but INDEX3 was more strongly related to plot-level ALC (not shown). As a result, rumple was excluded as a potential predictor variable. Lidar-derived vegetation metrics were generated with a 5 m horizontal cell size to facilitate spatial matching of lidar metrics to ALC estimates on plots that varied in size from 0.025 to 0.1 ha.

Numerous gridded topographic metrics were calculated from the DEM. Aspect was cosine transformed (Beers et al., 1966), slope

was calculated as percent, and two spatial scales of topographic position index (TPI30 and TPI300) were calculated as the difference between a cell's elevation and mean elevation of cells within a 30 and 300 m radius window. An intermediate scale TPI100 was also calculated with a 100 m radius window, but excluded from analyses due to its high correlation with fine and course topographic position (Electronic Supplemental Fig. 2). We also calculated distance to topographic exposure (TOPEX), a widely used metric for quantifying exposure and sheltering in relation to windthrow disturbance (Quine and White, 1998; Ruel et al., 2002). TOPEX was calculated for each pixel by generating concentric rings spaced in 50 m increments out to 2500 m from the focal pixel. In each of eight azimuthal classes the maximum vertical angle across concentric rings was calculated and summed for each focal pixel. Higher TOPEX values are more sheltered and lower values are more exposed. Because of the long distance used in calculating TOPEX, we buffered the DEM by 2500 m around the HJA with a DEM collected from an adjacent lidar acquisition to the north and a non-lidar derived 10 m DEM to the south. All lidar-derived vegetation and topography variables were generated at a 5 m cell size.

2.2.3. Harvest history, fire history, and soils data

Information about the year and type of all harvest activities at the HJA was modified from a previously compiled geospatial dataset (Lienkaemper, 2004). We estimated years since wildfire (YR_FIRE) and number of fires since 1500 (NFIRES) using the wildfire reconstruction for the HJA previously described by Seidl et al. (2012), which compiled detailed tree-ring based studies identifying the locations of thirteen wildfires since 1575 (Teensma, 1987; Weisberg and Swanson, 2003; Tepley, 2010). A map of soil physical properties (sand, silt, and clay fraction, and effective soil rooting depth) was derived from existing soil data for the HJA (Dyrness, 2005). Percent sand and clay fraction are strongly negatively correlated (Electronic Supplemental Fig. 2), so percent sand fraction was excluded from subsequent analyses. For additional information regarding harvest, fire, and soils datasets please see Appendix A.

2.2.4. Climate data

Climate data came from spatial grids of temperature, precipitation, and radiation previously developed for the HJA (Daly and Smith, 2005a,b; Daly and Rosentrater, 2005). Average annual temperature (TEMP) and annual precipitation (PRECIP) for the climatological period of 1980–89 were developed by interpolation of point station measurements to a spatial grid using the Parameter Estimates of Independent Slopes model (PRISM) that incorporates the influence of elevation on climate (Daly et al., 1994). The version of PRISM climate data we used is a localized variant giving spatial predictions based on a temporally limited set of weather station data from within the HJA, versus the much larger national PRISM data that is available for a longer time period (Daly et al., 2008). Native cell size of the climate data was 100 m, which was resampled to 25 m. Temperature and precipitation are highly correlated (see Electronic Supplemental Fig. 2), and correlation analysis as well as ecosystem simulations previously found temperature to be more important than precipitation in describing variation of forest C in the old-growth portion of the study area (Seidl et al., 2012). For these reasons, precipitation was removed as a potential explanatory variable in subsequent analyses. Elevation is often used as a proxy for climate variables in mountainous terrain (Whittaker, 1978), however the availability of spatially explicit climate data and the strong linear correlations between elevation and climate (see Electronic Supplemental Fig. 2) precluded the use of elevation in statistical analyses below.

2.3. Statistical analyses

2.3.1. Estimating and mapping ALC density using lidar data

All statistical analyses were conducted in the R statistical environment version 2.15.1 (R Development Core Team, 2012). A regression model of ALC was developed by relating plot estimates of ALC to lidar metrics of vegetation structure, following the approach taken by Seidl et al. (2012). The response variable was plot-based ALC (Mg ha^{-1}), cube-root transformed to address skewness. Lidar metrics were generated at a 5 m cell size because plots varied greatly in size and shape, and templates of 5 m cells were used to extract mean values of lidar metrics for areas that closely approximated the footprint of field plots. Since field plots were spatially clustered, they were divided into 42 spatially independent groups determined by a combination of visual assessment of geographic distances between plots and distinct landforms plots were located on. Potential predictor variables were the five previously described lidar metrics of vegetation height, cover, and vertical variability (H_{mean}, H_{var}, H_{95}, COV_2, COV_{40}, and INDEX3). To identify the best set of predictor variables, linear regressions were developed using the average cube-root transformed ALC for each of the 42 groups as the response variable. The best predictor variables were selected using a modified forward selection procedure. To account for the spatial clustering of plot data, final fit, coefficients, and standard errors of model coefficients were estimated using 100,000 iterations of a non-parametric bootstrap in which plots within spatially independent groups were re-sampled with replacement (Davison and Hinkley, 1997). We assessed model prediction by comparing observed versus predicted values, and residual versus observed values. We also assessed spatial variation in model fit by mapping model residuals of ALC for the 42 groups across the HJA, and then visually assessing the map for strong spatial patterns in model residuals. The average model coefficients from the bootstrap iterations were applied to the selected lidar predictor variables to create a map of cube root transformed ALC, which was back transformed into a map of ALC density (Mg ha^{-1}, 25 m cell).

2.3.2. Spatial autocorrelation of mapped ALC density

One of the statistical methods (Random Forest, see Section 2.3.5 below) used to quantify relationships between environmental variables and mapped ALC does not account for spatial autocorrelation, necessitating a sample of mapped ALC where sample points are not spatially autocorrelated. We quantified spatial autocorrelation by calculating omnidirectional empirical semivariograms of mapped ALC using the classical method of moments estimation implemented in the GeoR package for R (Ribeiro and Diggle, 2001). Computational constraints caused by the large number of cells within the ALC raster (213,570) necessitated random sampling of data. 10,679 cells (five percent of cells) were randomly sampled 20 times. Semivariograms were computed for each of these samples. Model parameters (range, partial sill, and nugget) of each sample semivariogram were calculated with an ordinary least squares parametric model using the Nelder–Mead algorithm (Nelder and Mead, 1965).

2.3.3. ALC density in relation to time since harvest and wildfire

Forest height, volume, biomass, and C often have non-linear relationships with forest age (McCardle and Meyer, 1930; Van Tuyl et al., 2005; Hudiburg et al., 2009). Given that relationships between ALC and forest age could be different between young versus old forests, we developed separate regression models to quantify the relationships between mapped ALC and stand age (YR_HARV in young managed forests, and YR_FIRE in old unmanaged forest). To minimize edge effects and small sections of

harvests intersecting the study area boundary, analysis of ALC and YR_HARV in young managed forests was limited to the mean mapped ALC in 135 harvest units containing at least twenty 25 m cells (1.25 ha). For old unmanaged forests, we calculated mean mapped ALC on a random sample of 114 square plots comprised of 9 × 9 25 m cells (5.0625 ha), spatially constraining plots so they didn't intersect harvested areas or different years since most recent fire. After visually assessing scatterplots of ALC and stand age, we compared three regression models of ALC in young managed forests (age^3, $age + age^3$, and $age + age^2 + age^3$) and two regressions of ALC in old unmanaged forests (age, log transformed age). The best models for young and old forests were determined based on adjusted R^2 values, as well as Akaike information criterion (AIC), AIC differences (ΔAIC), likelihood of a model given the data ($L(g_i|x)$, Akaike weights (w_i), and evidence ratios (w_1/w_2) following Burnham and Anderson (2002). Specifically, we choose the model with the highest adjusted R^2 and lowest AIC value. If multiple models had substantial empirical support (ΔAIC values of 0–2, Akaike weights greater than 0.2, and evidence ratios less than 2), the best model was chosen based on its approximation of ecologically realistic patterns of ALC in relation to years since disturbance. The best models for young and old forests were then used as the stand age explanatory variables in subsequent analyses below.

2.3.4. Random forest (RF) modeling of ALC in relation to environmental variables

To assess the relative importance of potential predictor variables on ALC, we calculated variable importance values using the random forest (RF) algorithm (Breiman, 2001; Liaw and Wiener, 2002). Mapped ALC density displayed strong spatial autocorrelation (mean semivariogram range of 471 m, Fig. 3). We addressed this by randomly sampling points with a minimum distance of 471 m using the rSSI function in the spatstat package (Baddeley and Turner, 2005). We additionally constrained sampling to at least 50 m from an edge between managed and unmanaged forests. Sampling resulted in 150 total points (35 managed and 115 unmanaged). Mean values for mapped ALC and potential predictor variables were extracted from square plots comprised of 3 × 3 25 m cells centered on each sampling point. As applied in this study, RF selected 1500 bootstrap samples, each containing two-thirds of the sampled cells. For each sample, RF generated a regression tree, then randomly selected only one-third of the predictor variables and chose the best partition from among those variables. To assess predictive power of the model, RF calculated an average from all the regression trees, which was used to predict ALC for the sampled cells not included in the bootstrap sample. The RF model was then used to calculate the importance values for each predictor variable as the percent increase in the mean squared error (MSE) in the predicted data when values for that predictor were permuted and all other predictors were left unaltered. We generated RF models and associated variable importance values for ALC in relation to environmental variables for: (1) 150 samples across managed and unmanaged forest in relation to 13 environmental variables (Table 1), (2) 115 samples across unmanaged forests in relation to the same variables above less HARVEST and including YR_FIRE, and (3) the 35 samples in managed forests in relation to the same 12 variables in (2) plus YR_HARV. By calculating variable importance values in these three different ways we were able to assess the relative importance of environmental variables on ALC across the entire study area, and separately for young managed and old unmanaged forests, respectively.

2.3.5. Sequential autoregressive (SAR) modeling of ALC in relation to environmental variables

In addition to RF analysis, we modeled ALC in relation to environmental variables using sequential autoregressive (SAR) modeling. We chose this complementary approach because of the lack of independence of mapped ALC values and the strong spatial structure of environmental variables, neither of which are explicitly accounted for in the RF analysis. In contrast to RF, SAR and other spatial regression modeling approaches incorporate the inherent spatial autocorrelation in response and environmental variables by using a spatial error term (Haining, 1993), resulting in more robust inferences than methods that do not account for spatial autocorrelation (Wimberly et al., 2009). SAR and similar spatial regression approaches have been increasingly used to analyze fire severity patterns inferred from satellite imagery and their underlying environmental determinants (Thompson et al., 2007; Wimberly et al., 2009; Prichard and Kennedy, 2013), as well as to predict forest biomass and productivity using forest inventory data (Ver Hoef and Temesgen, 2013), but we are unaware of attempts to apply these geostatistical methods to forest C density inferred from lidar data.

SAR models were constructed using the spautolm function from the spdep package in R (Bivand et al., 2013). SAR models were constructed separately for young managed and old unmanaged portions of the HJA because unmanaged cells had no assignment of years since harvest. Potential predictor variables (Table 1) were screened using box and whisker plots to examine relationships between predictor variables and ALC. YR_HARV and YR_FIRE were used as predictor variables of stand age for young and old forests, respectively. SAR models using different combinations of screened predictor variables were compared using AIC, and the final models were based on significance ($\alpha = 0.05$) of predictor variables and the lowest AIC values. Analyses were conducted on the full 25 m resolution mapped ALC dataset. The spatial neighborhood of cells in the inverse distance rule of the SAR spatial weights matrix was selected by choosing the neighborhood that minimized both SAR model AIC and residual spatial autocorrelation (Kissling and Carl, 2008; de Knegt et al., 2010). This was implemented by creating SAR models using eight different neighborhood distances (25–200 m in 25 m increments), and for each SAR model calculating AIC values and spatial autocorrelation of the SAR residual values using the moran.test function in the spdep package (Bivand et al.,

Table 1
List of potential environmental variables used in Random Forest (RF) and sequential autoregressive (SAR) models.

Type	Variable	Description
Topography	ASPECT	Cosine transformation of aspect (Beers et al., 1966)
	SLOPE	Slope (%)
	TPI30	Topographic position index, calculated as difference between a cell's elevation and mean elevation of cells within a 30 m radius window
	TPI300	Topographic position index, calculated as difference between a cell's elevation and mean elevation of cells within a 150–300 m radius window
	RAD	Annual mean daily solar radiation ($MJ\ m^{-2}\ d^{-1}$, Daly and Smith, 2005b)
	TOPEX	Topographic exposure
Soil	SOILDEPTH	Effective soil depth (m)
	SILT	Soil silt fraction (%)
	CLAY	Soil silt fraction (%)
Disturbance	YR_FIRE	Years since most recent fire (in relation to 2008 when lidar was collected)
	YR_HARV	Years since most recent harvest (in relation to 2008 when lidar was collected)
	NFIRES	Number of fires (including 1500 fire across entire HJA)
	HARVEST	Harvest binary indicator variable (yes/no)
Climate	TEMP	Mean annual temperature (C, Daly and Smith, 2005a)

2013). AIC values strongly supported a 50 m neighborhood distance, while spatial autocorrelation of SAR model residuals was comparable for both 25 m and 50 m neighborhood distances, so a 50 m neighborhood distance was used.

3. Results

3.1. Distributions and correlations of environmental variables

Environmental variables generally had the same range of values between young managed and old unmanaged forests (Electronic Supplemental Fig. 1), although there were important differences in frequency distributions for specific variables. Young managed forests tended to occur on lower elevation sites with higher annual mean temperature, more gradual slopes, intermediate topographic positions, and higher soil fractions of clay. Environmental variables displayed varying levels of correlation to each other in both young managed and old unmanaged forests (Electronic Supplemental Fig. 2). PRECIP and TEMP were highly correlated (Pearson $r = 0.88$), and both were highly correlated to elevation ($r = 0.83$–0.93). SAND and CLAY were also highly correlated to each other ($r = 0.88$–0.91), as well as to elevation ($r = 0.44$–0.56), PRECIP ($r = 0.33$–0.36), and TEMP ($r = 0.44$–0.50). The three different spatial scales of topographic position index (TPI30, TPI100, TPI300) were moderately to highly correlated with each other ($r = 0.41$–0.77), as were SLOPE and TOPEX ($r = 0.37$–0.41). YR_HARVEST was moderately correlated to elevation, as well as to TOPEX, SAND, CLAY, and TEMP ($r = 0.14$–0.32), with harvests more likely to occur at lower, warmer, and more sheltered sites with reduced sand and greater clay fraction. Finally, in old forests YR_FIRE was moderately correlated to TPI300 and TOPEX ($r = 0.25$–0.30), with fires most common on less sheltered ridges and mid slopes.

3.2. Modeling and mapping ALC density

The best regression to predict cube root transformed ALC included H_{95} and INDEX3 (Table 2, Fig. 1). Average adjusted R^2 for the final regression model across all bootstrapped samples was 0.754 (90% confidence interval of 0.687–0.806). Visual assessment did not find strong spatial patterns in model residuals of the back-transformed predicted ALC compared to observed ALC for the 42 spatially independent groups of plots (Electronic Supplemental Fig. 4). Applying the mean regression model coefficients (Table 2) to the gridded lidar explanatory variables, the mean and standard deviation of back transformed ALC was 302 ± 201 Mg ha^{-1} for the entire HJA, 364 ± 192 Mg ha^{-1} for old unmanaged forests, and 112 ± 60.6 5 Mg ha^{-1} for young managed forests of the HJA (Fig. 2). The mean range of the 20 semvariograms of mapped ALC was 471.46 m (Electronic Supplemental Table 1, Electronic Supplemental Fig. 3).

3.3. ALC density in relation to years since disturbance

Plantations ranged from 12 to 57 years old, and varied in size from 1.38 to 97.44 ha. The top ranked regression model of mapped ALC density in relation to age included the predictor variable YR_HARV^3 (Fig. 3, Electronic Supplemental Table 2). This model was significant at $P < 0.0001$ and had an adjusted R^2 of 0.59. One other model had substantial empirical support (ΔAIC = 1.02), but had an ecologically unrealistic model form where ALC remained constant or increased as YR_HARV declined from 20 years old to zero. Time since last wildfire ranged from 55 to 507 years, with estimated areas within the HJA ranging from 20.31 to 4372.88 ha (although this does not include areas of fires occurring outside the HJA watershed). The top ranked model of ALC in relation to time since fire included the predictor variable log(YR_FIRE) (Fig. 3, Electronic Supplemental Table 2). This model was significant at $P < 0.0001$ and had an adjusted R^2 of 0.11. No other models for old unmanaged forests had substantial levels of empirical support (ΔAIC $\leqslant 2$). Compared to young managed forests, ALC in old unmanaged forests was highly variable with respect to stand age, and the model form indicates an asymptote of ALC beyond 500 years old.

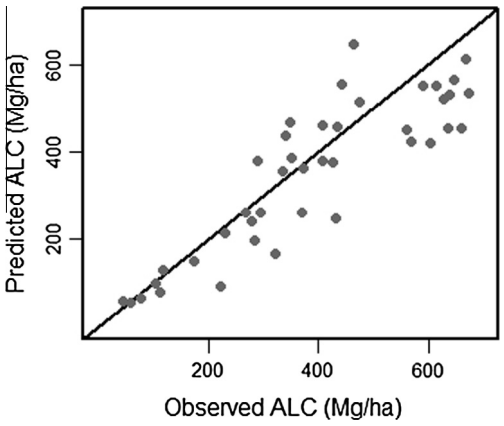

Fig. 1. Observed versus predicted aboveground live carbon (ALC). Gray points represent the mean observed and predicted ALC for each of 42 spatially independent groups of plots. 1:1 line in black. Predicted ALC values are back transformed from cubed root ALC in the regression model.

3.4. Random forest models of ALC density in relation to environment variables

RF models explained 54%, 65%, and 34% of the variability in ALC density across the entire HJA, young managed forests, and old unmanaged forests, respectively. Across the entire HJA, HARVEST was the dominant predictor variable, reducing MSE by over 90% (Fig. 4). Within young managed forests, TEMP and YR_HARV were the most important predictor variables (reducing MSE by 32% and 31%), with only one other predictor variable (CLAY) reducing MSE by at least 10%. The RF model for old unmanaged forests explained the least amount of variability in ALC. TEMP was its most important predictor variable, and two other predictor variables (CLAY and TOPEX) each reducing MSE by at least 10%. More predictor variables appear to be important in explaining variation in ALC for old unmanaged versus young managed forests, while both years since wildfire (YR_FIRE) and the number of wildfires (NFIRES) were not important predictor variables in old unmanaged forests (reducing MSE by 6% and 2%, respectively).

3.5. SAR models of ALC density in relation to environment variables

SAR models explained 79% and 65% of the variability in ALC density across young managed forests and old unmanaged forests, respectively. Predicted ALC density had strong spatial correspondence to lidar-derived maps of ALC density, with high and low ALC values visually similar between SAR predicted and lidar mapped values (Fig. 5). Residuals from the SAR models tended to

Table 2
Mean parameter estimates and 90% confidence internal (CI) for the 100,000 bootstrapped regression models of aboveground live carbon (ALC) density in relation to lidar metrics vegetation structure.

Parameter	Estimate	Lower 90% CI	Upper 90% CI
Intercept	1.2496240	1.0235000	1.4037830
H_{95}	0.0219194	0.0135175	0.0337647
INDEX3	−0.0000049	−0.0000106	−0.0000007

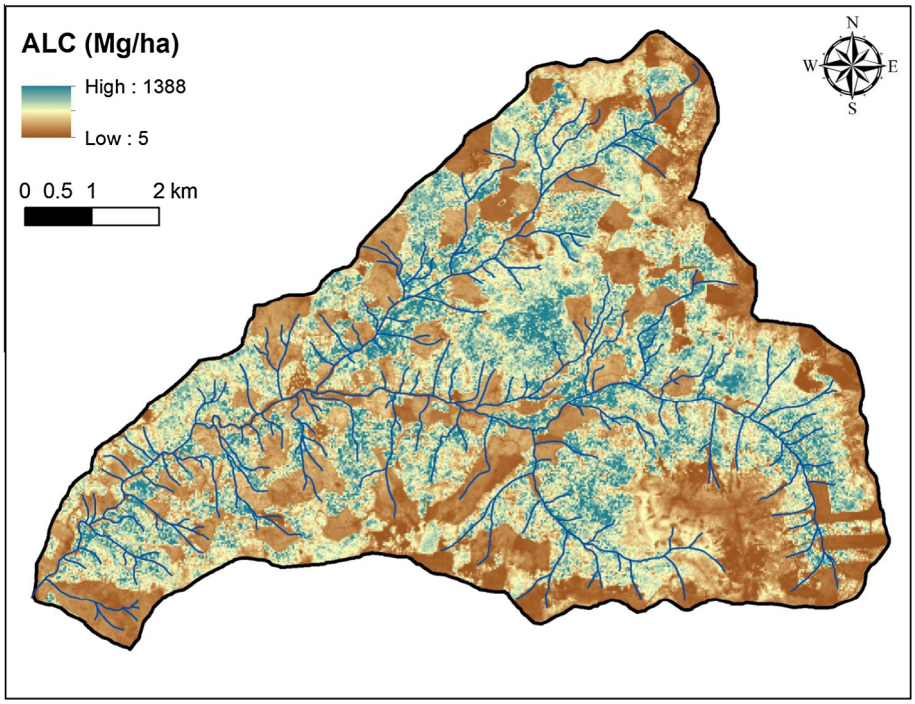

Fig. 2. Study area map of back transformed predicted aboveground live carbon (ALC). Streams depicted in blue. Note: cell size is 25 m. (For interpretation of the references to color in this figure legend, the reader is referred to the web version of this article.)

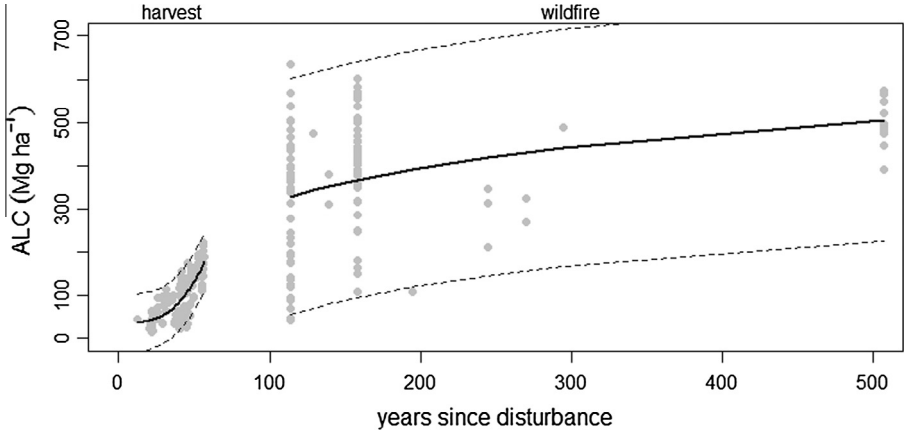

Fig. 3. Aboveground live carbon (ALC) in relation to years since harvest and wildfire. Model fit (black solid line) and 95% confidence interval (gray dashed lines) are for best models of ALC in relation to years since harvest (YR_HARVEST) and years since wildfire (YR_FIRE) in 135 harvest units and 114 unmanaged sample polygons (see methods section for description of harvest units and polygon sampling).

over predict ALC in old unmanaged forests (Electronic Supplemental Fig. 5). However, when assessing SAR model proportional residuals (i.e., as the percentage difference between model residuals and lidar mapped ALC), the greatest percentage difference was not between young and old forests, but rather over prediction of ALC in unmanaged areas associated with meadows and rock outcrops (Electronic Supplemental Fig. 6). Significant predictor variables in common between SAR models of young managed and old unmanaged forests included: TEMP, TPI30, TPI300, and CLAY (Table 3). The best SAR model for young managed forests also included YR_HARVEST, SLOPE, and YR_FIRE, while the SAR model for old unmanaged forests also included RAD, TOPEX, and SILT predictor variables. YR_FIRE was retained in the SAR model for old unmanaged forests, but it only had a suggestive relationship with ALC ($P = 0.07$). Other predictor variables that were not significant predictors in SAR models included ASPECT, NFIRES, and SOILDEPTH.

3.6. ALC density in relation to climate, topography, soils, and disturbance history in young versus old forests

Temperature was a significant predictor of ALC density in RF and SAR models for both young and old forests. ALC in old unmanaged forests steadily increased with increasing temperatures until reaching a plateau around 8.5 °C, after which ALC did not vary with temperature until a slight decline in ALC above 10 °C (Fig. 6). ALC in young managed forests also increased with increasing temperature, but did not display the plateau in ALC as found in unmanaged forests. ALC in young unmanaged and old managed forests declined with increased topographic position at both fine (TPI30)

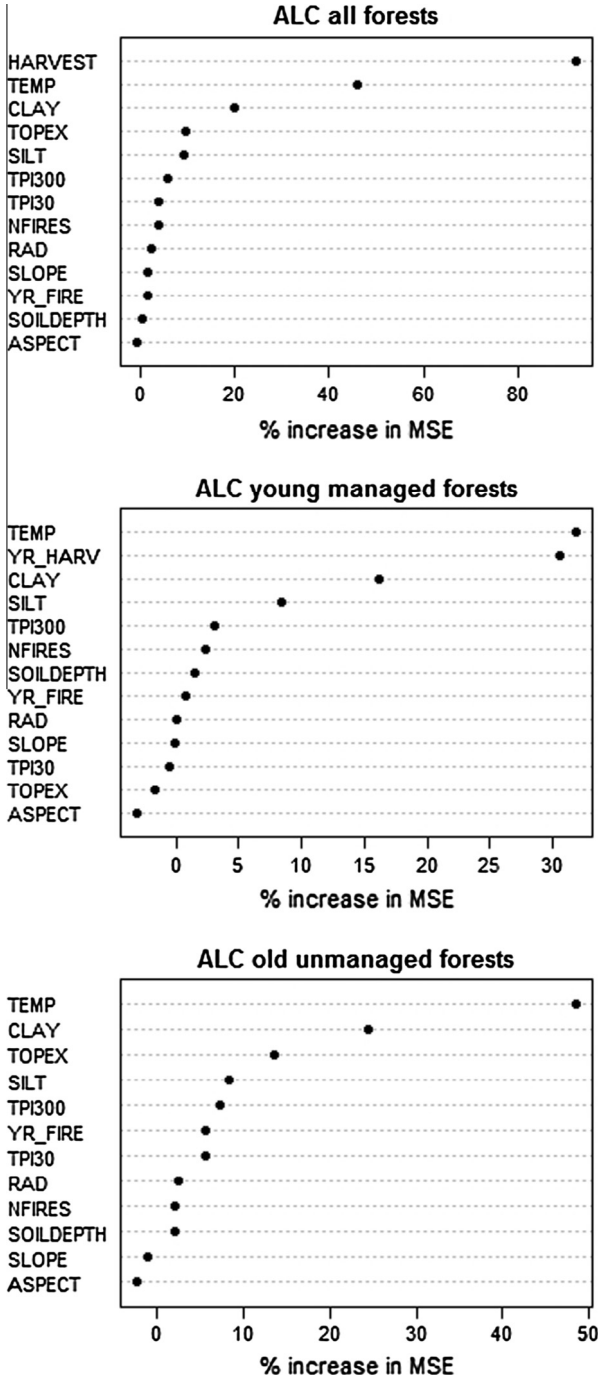

Fig. 4. Variable importance plots for environmental variables from random forests models of ALC for 150 sample plots across the entire HJA landscape (upper left), 35 plots in managed forests (upper right), and 115 plots in unmanaged forests (lower right). See Table 1 for descriptions of environmental variables.

and coarse (TPI300) scales, but this relationship was also more pronounced in unmanaged forests. CLAY was a significant predictor in RF and SAR models for both young managed and old unmanaged forests, yet it's relationship with ALC was highly variable.

In addition to the significant variables in SAR models for both young and old forests, two additional variables (YR_HARVEST, YR_FIRE, and SLOPE) were significant in the SAR model for young managed forests, while three additional variables (RAD, TOPEX, SILT) were significant and one suggestive (YR_FIRE) for old unmanaged forests (Table 3, Fig. 6). ALC in young managed forests steadily increased with YR_HARVEST, and declined with increasing SLOPE. The influence of YR_FIRE in young managed forests appears to be driven by two recent small fires (1952 and 1935), and older fires do not appear to influence ALC (Fig. 6). In old unmanaged forests, ALC was variable but increased slightly with greater YR_FIRE and SILT, was highest at higher TOPEX values (more sheltered), and was lower at the highest and lowest RAD values.

4. Discussion

In both RF and SAR analyses, climate, topography, and soil conditions were all important drivers of forest ALC density, and these drivers varied significantly between young managed vs. old unmanaged forests. Below, patterns of forest ALC density and environmental relationships are discussed in terms of (1) Complementary value of RF and SAR analyses, (2) dominant environmental drivers of ALC density at the landscape scale, (3) differences in environmental drivers of ALC between young managed forests and old unmanaged forests, (4) the limitations of our study, and (5) implications of high spatial variability of forest ALC density in complex mountain terrain.

4.1. Complementary value of RF and SAR analyses

Lidar data enabled the development of high resolution maps of forest ALC density across managed and unmanaged forests, allowing us to quantify spatial variation of ALC and its underlying environmental determinants. By examining the relationships between ALC density and environmental drivers using complementary statistical methods (RF and SAR), we were able to make stronger inferences about the importance of environmental variables in young versus old forests, while placing results within the context of strengths and weakness of each statistical method. RF's primary strength in the context of this study is the ability to model complex interactions among environmental variables (Prasad et al., 2006; Cutler et al., 2007). This strength over regression modeling (including SAR) may be especially important in complex mountainous terrain, where strong interactions between climate, physiography, and disturbance history occur. Additionally, RF variable importance values can be used to subjectively identify and interpret ecologically meaningful predictor variables. However, RF is not well suited to traditional statistical inference, variable selection, or variable significance, and RF models were developed from a small spatially constrained sample of the study landscape to address concerns of spatial autocorrelation. In contrast, SAR models incorporate a spatial error term, explicitly addressing spatial autocorrelation, while indirectly including unmeasured but spatially structured environmental variation (Haining, 1993). SAR models used a complete census of mapped ALC for the study area, which may enable detection and quantification of more subtle interactions between ALC and environmental variables versus RF analyses based on samples. Additionally, SAR can be used for more traditional statistical inference, variable selection, and quantifying variable significance compared to RF.

4.2. Dominant drivers of forest ALC density

Timber harvesting was the single most important driver of variation in forest ALC density, despite occurring on only 23% of the landscape. This is not surprising given the many centuries it can take to reach the upper bounds of forest ALC density in the region (Hudiburg et al., 2009; Seidl et al., 2012), and largely mature and old-growth forest conditions at the HJA prior to initiation of harvesting in the 1950s. After forest harvesting, annual temperature was the next most important driver of variation in forest ALC density in both models for both young managed and old unmanaged

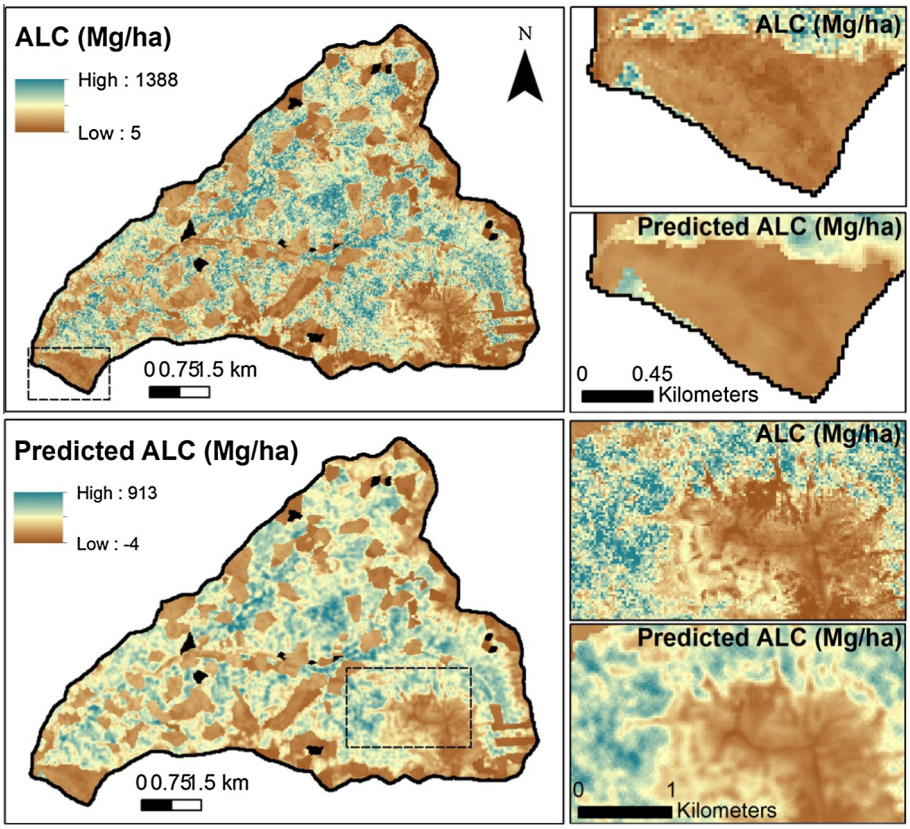

Fig. 5. Maps of aboveground live carbon (ALC) from lidar and sequential autoregressive (SAR) model predictions for the HJA study area. Dashed rectangles in maps on the left correspond to enlarged areas on the right. Map cell size is 25 m. Black areas denote partial harvests with variable tree retention that were excluded from SAR analysis. (For interpretation of the references to color in this figure legend, the reader is referred to the web version of this article.)

Table 3
Coefficients for selected SAR models of aboveground live carbon (ALC) in relation to environmental variables.

	Young managed forests (pseudo R^2 = 0.79, AIC = 230,041)				Old unmanaged forests (pseudo R^2 = 0.65, AIC = 959,554)			
	Estimate	SE	*Z* value	*P*	Estimate	SE	*Z* value	*P*
Intercept	−151.1340	10.8219	−13.9656	0.0000	−351.5887	29.5312	−11.9057	0.0000
YR_HARVEST	0.0004	0.0000	24.9743	0.0000	–	–	–	–
YR_FIRE	−2.5369	1.2685	−1.9999	0.0455	5.1597	2.9314	1.7602	0.0784
SLOPE	0.1004	0.0199	5.0458	0.0000		–	–	–
TPI30	−1.9260	0.2098	−9.1811	0.0000	2.4587	0.5146	4.7782	0.0000
TPI300	−0.1944	0.0337	−5.7707	0.0000	−0.6647	0.1026	−6.4755	0.0000
RAD	0.8515	0.4070	2.0921	0.0364	4.6123	0.9978	4.6226	0.0000
CLAY	0.3126	0.0665	4.7035	0.0000	−0.8035	0.2062	−3.8974	0.0001
TOPEX	–	–	–	–	0.6172	0.0690	8.9400	0.0000
SILT	–	–	–	–	2.2778	0.2613	8.7170	0.0000
TEMP	0.2334	0.0089	26.0881	0.0000	0.5206	0.0220	23.6802	0.0000

forests. The impacts of climate on vegetation productivity have been well studied at regional to global scales (Churkina and Running, 1998; Nemani et al., 2003; Latta et al., 2009). However, in this study we found climate mediated by complex mountain terrain can result in high variation of the upper bounds of forest ALC density across relatively short distances. For example, in old unmanaged forests at the HJA, median ALC density declined by more than a factor of three (410–130 Mg ha^{-1}) across a horizontal distance of just a few hundred meters in association with a 4.73 °C decline (10.69–5.96 °C) in annual temperature and a 650–1400 m increase in elevation (Fig. 6, Electronic Supplemental Fig. 7). ALC density in young managed forests also declined with reduced temperature (and thus increased elevation) across relatively short distances, but the magnitude of this decline was less than in old unmanaged forests. This difference in the magnitude of ALC response to temperature may result from compounding effect of site productivity over time (i.e., ALC as the integral of annual growth over time). Using correlation analysis and simulation models, Seidl et al. (2012) quantified similar fine grained variation in forest total ecosystem carbon (TEC), but found solar radiation to be a more important driver than temperature in old unmanaged forests. These differences may in part arise from different aspects of carbon studied (ALC vs. TEC) and fundamentally different analyses, with Seidl et al. (2012) considering the integral effect of environmental drivers over a 500 year period using process-based simulations.

After harvest history and climate, soil texture (fraction of clay) was important in analyses for both young managed and old unmanaged forests. Many soil physical characteristics (i.e., soil depth, texture, water holding capacity, etc.) influence forest

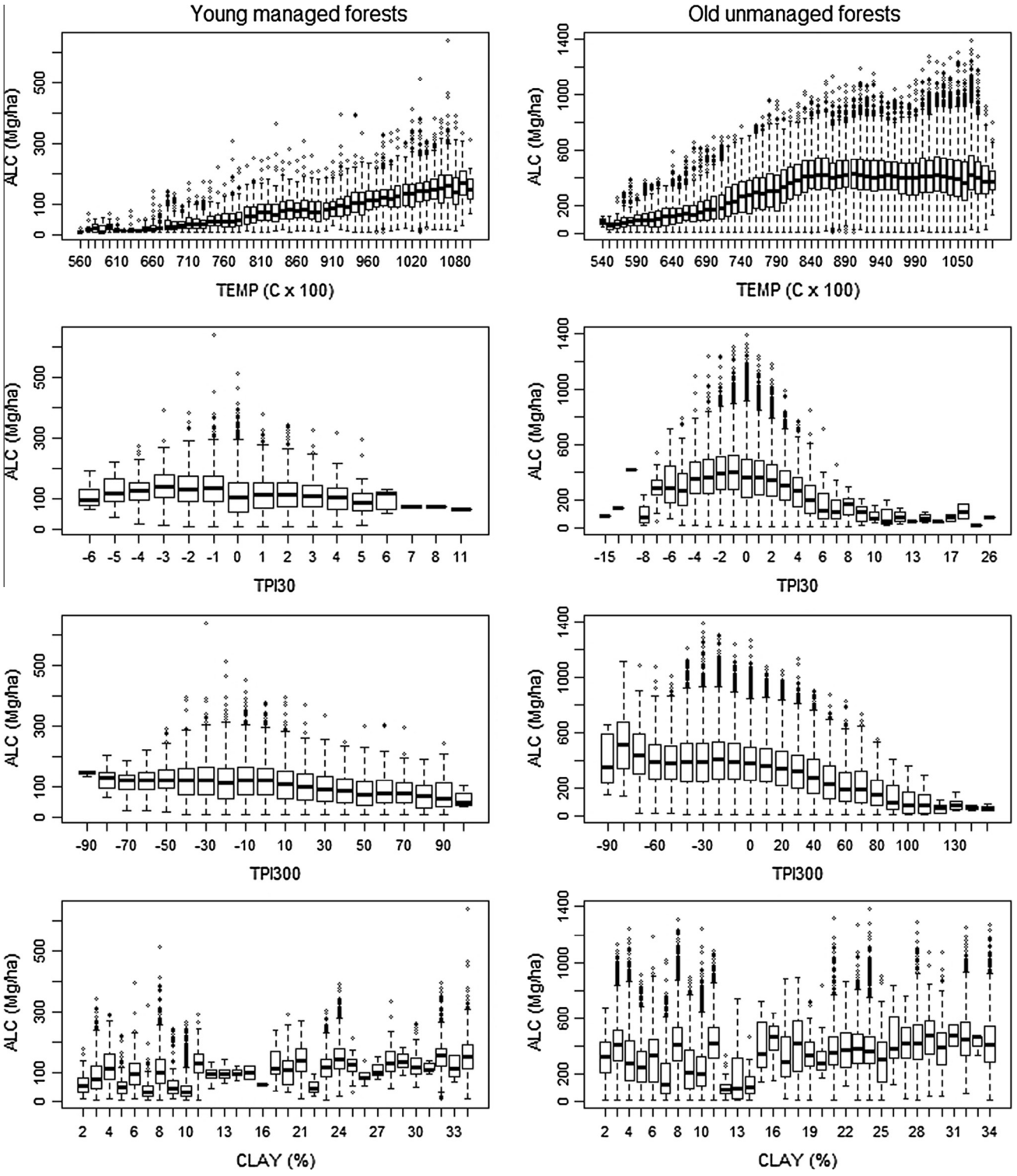

Fig. 6. Boxplots of aboveground live carbon (ALC) in relation to TEMP, TPI30, TPI300, and CLAY for young managed and old unmanaged forests. Boxplots of aboveground live carbon (ALC) in relation to YR_HARV, YR_FIRE, and SLOPE for young managed forests; and YR_FIRE, RAD, TOPEX, and SILT in old unmanaged forests.

productivity (Binkley and Fisher, 2012; Meyer et al., 2007), and these characteristics vary with topographic position (Tromp-van Meerveld and McDonnell, 2006; Griffiths et al., 2009). RF and SAR analyses had less agreement on important topographic variables, although both analyses indicated an increased importance of TOPEX in old forests. Topographic variables, such as TPI30 and TPI300, may reflect both microclimate and other factors that vary with topography such as soils, exposure to wind, and wildfire (Tepley et al., 2013) and windthrow (Sinton et al., 2000; Kramer et al., 2001). Variation in temperature is largely driven by elevation (Daly et al., 1994, Electronic Supplemental Fig. 2), and elevation is often used as a proxy to represent complex environmental gradients (Whittaker, 1978). However, elevation alone does not capture additional topographic context such as topographic shading,

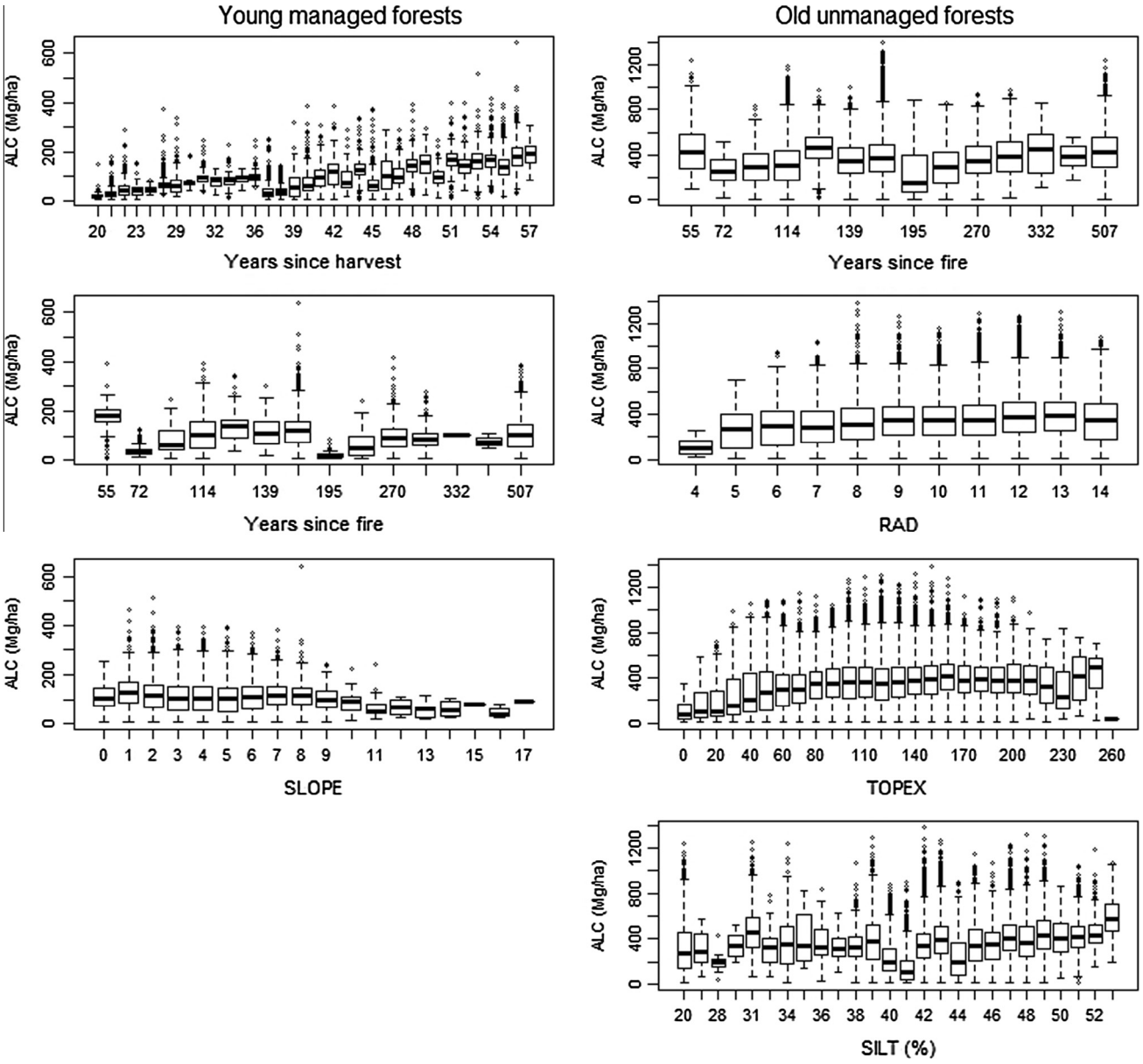

Fig. 6 (*continued*)

relative radiation, local depressions, and valley constrictions that can mediate temperatures (Lookingbill and Urban, 2003; Daly et al., 2010).

4.3. Environmental drivers of ALC vary between young managed and old unmanaged forests

The relationship between ALC and stand age was stronger in young forests than in older forests, which also displayed an asymptote for ALC beyond 500 years. Across both strata, ALC development with age is consistent with general trends of biomass recovery after disturbance (Bormann and Likens, 2012). However, we were unable to characterize the trend between ages 57 and 106, a short period when ALC may increase by 50% or more to reach the levels found in older forests. Both mean annual growth culmination and transitions between the developmental stages of biomass accumulation and maturation are known to occur between stand ages of 70–150 years in these forests (Curtis et al., 1974; Franklin et al., 2002), leading us to believe that in combination, the two ALC-age regressions are capturing the general trend of ALC over time.

For young managed forests, years since harvest, along with large-scale gradients of climate, soils, and topography were important in both models. RF and SAR model fit was better in young managed versus old unmanaged forests, and there was good visual agreement between observed ALC and SAR predictions. In old unmanaged forests, moderate to large scale gradients of climate, soils, and topography still exerted a strong influence on ALC density, while model fit was lower for both RF and SAR models compared to young managed forests. Additionally, SAR predictions of ALC did not appear to capture fine-scale variation in ALC that is more prevalent in old unmanaged forests (Fig. 5). Differences between models of young and old forests are consistent with what is known about the structural development and underlying processes in forests of the region, and may indicate a shift in drivers of forest ALC density associated with changes in vegetation structure as forests age, from large-scale exogenous factors associated with forest productivity to increased importance of finer-scale

processes including gap dynamics and the establishment and growth of shade-tolerant species (Spies et al., 1990; Franklin et al., 2002; Seidl et al., 2012). Young managed stands at the HJA are 12–57 years old, and are largely in canopy closure and biomass accumulation/competitive exclusion stages of stand development (sensu Franklin et al., 2002). In these developmental stages, mortality is largely density-dependent and occurs at stand scales, although gap-forming processes and structural complexity more often associated with older forests can occur (Lutz and Halpern, 2006). In contrast, older forests are typically characterized by (1) a shift from density dependent to density independent overstory mortality, (2) senescence of overstory trees, and (3) establishment and growth of shade-tolerant trees. The accumulation of finer-scale and spatially aggregated mortality over decades and centuries is a likely cause of the fine-scale spatial heterogeneity in the ALC density of old forests, which is not predicted by our models. Furthermore, older forests in the region have higher tree species richness due to establishment of shade-tolerant species, and this increased species richness has been associated with increased ALC density (Seidl et al., 2012), likely as a result of complementary resource use where large shade tolerant conifer species co-occur in mid and lower canopy positions with emergent, long-lived shade intolerant species

While years since harvest was strongly associated with forest ALC density in young managed forests, years since fire was only weakly associated with ALC density in old unmanaged forests, and the number of fires on a given site over time was not a significant predictor of forest ALC density. Fires differ strongly from harvesting in their impact on vegetation and ALC dynamics, and fires are much more heterogeneous in their impact compared to management (Franklin et al., 2002). The fire regime in Douglas-fir/western hemlock forests that dominate the HJA has typically been viewed as low frequency, high severity, stand replacing disturbance (Munger, 1930; Franklin et al., 2002). However, relatively little of the HJA has experienced stand replacing fire in the 20th century, making it impossible to compare young managed and young unmanaged stand development within the study area. The most recent fires occurred in the mid to late 1800s and were generally not stand replacing. Such mixed-severity events may be more important in the region than previously thought, resulting in more complex trajectories of structural development than suggested by traditional conceptual models (Weisberg, 2004; Tepley et al., 2013). Additionally, remnant old-growth trees resulting from non-stand replacing fires likely enhance the recovery of forest C density (Seidl et al., 2014). Some of the variation in ALC density that we found could be indicative of these non-stand replacing fires. However, our fire history maps are relatively coarse and subject to considerable uncertainty, therefore smaller patches of younger forest created by past fires would be difficult to delineate from historical aerial photography and dendroecology. Consequently, we may be underestimating the effect of these partial disturbances on variation in ALC density here (see discussion of study limitations below).

4.4. Study limitations

We only examined ALC density, and it's important to note that ALC may only represent approximately half of the total ecosystem carbon stores in old growth forests of the region (Smithwick et al., 2002). Furthermore, partitioning of different carbon stores and fluxes (i.e., above versus belowground C, primary production versus respiration, etc.) can vary across regional climate gradients and disturbance history (Law et al., 2004). Quantifying these other C stores and fluxes and their spatial variability is problematic using remotely sensed data and beyond the scope of this study, where we focus only on ALC.

Our study was conducted at the HJA, a long-term experimental forest with a wealth of information regarding forest management, vegetation, disturbance history, climate, topography, and soils. However, there are many inherent limitations in the available data that restricted analyses and the strength of inference associated with our findings. The empirical relationship between lidar and field plots used to map forest ALC density was strong, but as noted by Seidl et al. (2012), these plots and their sampling schemes were designed for a variety of other purposes and not specifically for developing models of forest ALC. Additionally, there are multiple sources of sampling, measurement, and model misspecification errors that can influence forest biomass (and therefore ALC) estimation (Temesgen et al., 2015). Furthermore, soil physical characteristics were collected at a sampling density and spatial grain that is likely to miss fine-grained heterogeneity of soil conditions varying with topography, while many fine-grained environmental factors (rock outcrops, seepages, streams, etc.) were not accounted for explicitly. As a study focused on how topography and disturbance history influenced C density, aspects of stand development and succession such as species composition and diversity were not included, nor were they available with the accuracy required to be included in analyses. Yet species diversity and structural complexity likely explain a large faction of ALC not described by environmental factors (Seidl et al., 2012). While the study had detailed information about past management and wildfires, important information was not available for either disturbance type. For instance, spatially explicit data were not available for post-harvest management (site preparation, planting density, and regeneration success). Findings that suggest the importance of non-stand replacing fires must be placed in the context of fire reconstruction data, which lacked information regarding variability of fire severity within fires or locations of old-growth remnants. Furthermore, data on small-scale disturbances such as windthrow or insect mortality were not available, but those disturbances are likely to also contribute to the variation in ALC density at the scale of analysis. While differences in explanatory power and significant environmental variables between young and old forest have strong basis in known ecological patterns and process, inferences regarding difference in explanatory power may be weakened by the smaller overall gradient in ALC in the young managed forests, resulting in less variation of ALC to explain in statistical models compared to old forests. Overall, the considerably reduced explanatory power of our analyses in old-growth forests compared to young managed forests suggests that alternative tools and approaches (such as using simulation modeling as a diagnostic tool, Seidl et al., 2012) are of value in exploring the complexities of C cycling in old-growth forest ecosystems.

4.5. Conclusions

We found that complex mountain terrain strongly influenced ALC density, and these relationships differ between young and old forests. These findings have important implications for scaling up plot-level data to landscape and regional scales, as well as for modeling the spatiotemporal dynamics of forest carbon cycling at these scales. Regional-scale studies may miss important spatial variation in the upper bounds of forest C density in complex mountain terrain. Our study indicates that landscape-scale variation of climate, topography and soils exerts strong influences on C density and that the relationship can differ between younger managed forests and older unmanaged forests. Scaling and modeling applications that do not take this into consideration may overestimate forest C storage, because they underestimate environmental constraints in young forests and heterogeneous landscapes (cf. Seidl et al., 2013). Using large regional inventory plot networks may in part reduce these concerns by providing robust regional estimates

of forest C density and its variation with stand age (Hudiburg et al., 2009), but it is unknown how well these plot networks represent multi-scale gradients of environmental factors and management history that influence spatial variability of forest C density (Bradford et al., 2010).

Acknowledgements

Support for this research was provided by the H. J. Andrews Experimental Forest and the National Science Foundation Long-Term Ecological Research (LTER) program (NSF DEB 0823380). RS acknowledges support from the Austrian Science Fund FWF (grant P 25503-B16) and an EC Marie Curie Career Integration Grant (PCIG12-GA-2012-334104). Vegetation data sets were provided by the HJ Andrews Experimental Forest research program, funded by the National Science Foundation's Long-Term Ecological Research Program (NSF DEB 0823380), US Forest Service Pacific Northwest Research Station, and Oregon State University.

Appendix A. Harvest history, fire history, and soils data

Information about the year and type of all harvest activities at the HJA was modified from previously compiled geospatial dataset (Lienkaemper, 2004). This dataset was originally developed using harvest records and historical aerial photographs, but image distortions from topographic effects and spatial registration errors resulted in incorrect locations of harvest boundaries. We corrected harvest boundaries by overlaying the lidar-derived grid of 95th percentile vegetation height (H_{95}) on top of the original harvest dataset, and manually retraced harvest boundaries. Corrected harvest polygons were then rasterized to a 25 m cell size to create a binary harvest variable (HARVEST) and a continuous variable of years since harvest (YR_HARV). Majority of harvests were clear-cuts, although partial thinning with variable tree retention occurred on 53 ha, and these partial thinnings were excluded from our analyses. We estimated years since wildfire (YR_FIRE) and number of fires since 1500 (NFIRES) using the wildfire reconstruction for the HJA previously described by Seidl et al. (2012), which compiled detailed tree-ring based studies identifying the locations of thirteen wildfires since 1575 (Teensma, 1987; Weisberg and Swanson, 2003; Tepley, 2010). In addition, aerial photos from the 1950s and the lidar data from 2008 were used to corroborate and amend the last 100 years of the tree-ring based fire reconstructions. Seidl et al. (2012) assigned severity classes to individual fires based on the work of Weisberg (1998). However, in our study we did not assign severity classes to wildfires, because of their often high intra-fire spatial variability (Perry et al., 2011), and the inability to generate a spatially explicit characterization of fire severity classes from tree-ring data. Finally, Seidl et al. (2012) probabilistically modeled areas likely to have not burned at all in the past 500 years based on the work of Tepley (2010), but we excluded this information because confirming all locations of remnant unburned forests was beyond the scope of this study. A map of soil physical properties (sand, silt, and clay fraction, as well as effective soil rooting depth) was derived from existing soil data for the HJA (Dyrness, 2005). Soil data was rasterized, missing data derived using ordinary kriging, and resampled to a 25 m cell size as described in Seidl et al. (2012).

Appendix B. Supplementary material

Supplementary data associated with this article can be found, in the online version, at http://dx.doi.org/10.1016/j.foreco.2016.01.036.

References

Asner, G.P., Mascaro, J., 2014. Mapping tropical forest carbon: calibrating plot estimates to a simple LiDAR metric. Remote Sens. Environ. 140, 614–624.
Asner, G.P., Powell, G.V.N., Mascaro, J., Knapp, D.E., Clark, J.K., Jacobson, J., Kennedy-Bowdoin, T., Balaji, A., Paez-Acosta, G., Victoria, E., Secada, L., Valqui, M., Hughes, R.F., 2010. High-resolution forest carbon stocks and emissions in the Amazon. Proc. Natl. Acad. Sci. 107, 16738–16742.
Assmann, E., Franz, F., 1963. Vorläufige Fichten-Ertragstafel für Bayern 1963. Institut für Ertragskunde der Forslichen Forschungsanstalt.
Baccini, A., Friedl, M., Woodcock, C., Warbington, R., 2004. Forest biomass estimation over regional scales using multisource data. Geophys. Res. Lett. 31.
Baddeley, A., Turner, R., 2005. Spatstat: an R package for analyzing spatial point patterns. J. Stat. Softw. 12, 1–42.
Baldocchi, D., 1997. Flux footprints within and over forest canopies. Bound.-Layer Meteorol. 85, 273–292.
Baldocchi, D., Falge, E., Gu, L., Olson, R., Hollinger, D., Running, S., Anthoni, P., Bernhofer, C., Davis, K., Evans, R., 2001. FLUXNET: a new tool to study the temporal and spatial variability of ecosystem-scale carbon dioxide, water vapor, and energy flux densities. Bull. Am. Meteorol. Soc. 82, 2415–2434.
Baraloto, C., Rabaud, S., Molto, Q., Blanc, L., Fortunel, C., Herault, B., Davila, N., Mesones, I., Rios, M., Valderrama, E., 2011. Disentangling stand and environmental correlates of aboveground biomass in Amazonian forests. Glob. Change Biol. 17, 2677–2688.
Beers, T.W., Dress, P.E., Wensel, L.C., 1966. Notes and observations: aspect transformation in site productivity research. J. Forest. 64, 691–692.
Berenguer, E., Ferreira, J., Gardner, T.A., Aragão, L.E.O.C., De Camargo, P.B., Cerri, C.E., Durigan, M., Oliveira, R.C.D., Vieira, I.C.G., Barlow, J., 2014. A large-scale field assessment of carbon stocks in human-modified tropical forests. Glob. Change Biol. 20, 3713–3726.
Binkley, D., Fisher, R., 2012. Ecology and Management of Forest Soils. John Wiley & Sons.
Bivand, R., Altman, M., Anselin, L., 2013. Package 'spdep'.
Bormann, F.H., Likens, G., 2012. Pattern and Process in a Forested Ecosystem: Disturbance, Development and the Steady State based on the Hubbard Brook Ecosystem Study. Springer Science & Business Media.
Bradford, J.B., 2011. Divergence in forest-type response to climate and weather: evidence for regional links between forest-type evenness and net primary productivity. Ecosystems 14, 975–986.
Bradford, J.B., Weishampel, P., Smith, M.-L., Kolka, R., Birdsey, R.A., Ollinger, S.V., Ryan, M.G., 2010. Carbon pools and fluxes in small temperate forest landscapes: variability and implications for sampling design. For. Ecol. Manage. 259, 1245–1254.
Breiman, L., 2001. Random forests. Mach. Learn. 45, 5–32.
Bunker, D.E., DeClerck, F., Bradford, J.C., Colwell, R.K., Perfecto, I., Phillips, O.L., Sankaran, M., Naeem, S., 2005. Species loss and aboveground carbon storage in a tropical forest. Science 310, 1029–1031.
Burnham, K.P., Anderson, D.R., 2002. Model Selection and Multi-Model Inference: A Practical Information-Theoretic Approach. Springer Verlag.
Chen, J.M., Ju, W., Cihlar, J., Price, D., Liu, J., Chen, W., Pan, J., Black, A., Barr, A., 2003. Spatial distribution of carbon sources and sinks in Canada's forests. Tellus B 55, 622–641.
Churkina, G., Running, S.W., 1998. Contrasting climatic controls on the estimated productivity of global terrestrial biomes. Ecosystems 1, 206–215.
Curtis, R.O., Herman, F.R., DeMars, D.J., 1974. Height growth and site index for Douglas-fir in high-elevation forests of the Oregon-Washington Cascades. For. Sci. 20, 307–316.
Cutler, D.R., Edwards Jr., T.C., Beard, K.H., Cutler, A., Hess, K.T., Gibson, J., Lawler, J.J., 2007. Random forests for classification in ecology. Ecology 88, 2783–2792.
Daly, C., Rosentrater, L., 2005. Average Monthly and Annual Temperature Spatial Grids (1980–1990), Andrews Experimental Forest. Long-Term Ecological Research. Forest Science Data Bank, Corvallis, OR. <http://andrewsforest.oregonstate.edu/data/abstract.cfm?dbcode=MS028&topnav=97> (accessed August 21, 2015).
Daly, C., Smith, J., 2005a. Mean Monthly Maximum and Minimum Air Temperature Spatial Grids (1971–2000), Andrews Experimental Forest. Long-Term Ecological Research. Forest Science Data Bank, Corvallis, OR. <http://andrewsforest.oregonstate.edu/data/abstract.cfm?dbcode=MS029&topnav=97> (accessed August 21, 2015).
Daly, C., Smith, J., 2005b. Radiation Spatial Grids, Andrews Experimental Forest. Long-Term Ecological Research. Forest Science Data Bank, Corvallis, OR. <http://andrewsforest.oregonstate.edu/data/abstract.cfm?dbcode=MS033&topnav=97> (accessed August 21, 2015).
Daly, C., Halbleib, M., Smith, J.I., Gibson, W.P., Doggett, M.K., Taylor, G.H., Curtis, J., Pasteris, P.P., 2008. Physiographically sensitive mapping of climatological temperature and precipitation across the conterminous United States. Int. J. Climatol. 28 (15), 2031–2064.
Daly, C., Conklin, D.R., Unsworth, M.H., 2010. Local atmospheric decoupling in complex topography alters climate change impacts. Int. J. Climatol. 30, 1857–1864.
Daly, C., Neilson, R.P., Phillips, D.L., 1994. A statistical-topographic model for mapping climatological precipitation over mountainous terrain. J. Appl. Meteorol. 33, 140–158.
Davison, A., Hinkley, D., 1997. Bootstrap Methods and their Application. Cambridge University Press, Cambridge, UK, p. 193.

De Knegt, H., Van Langevelde, F., Coughenour, M., Skidmore, A., De Boer, W., Heitkönig, I., Knox, N., Slotow, R., Van der Waal, C., Prins, H., 2010. Spatial autocorrelation and the scaling of species–environment relationships. Ecology 91, 2455–2465.
Dobrowski, S.Z., Abatzoglou, J.T., Greenberg, J.A., Schladow, S., 2009. How much influence does landscape-scale physiography have on air temperature in a mountain environment? Agric. For. Meteorol. 149, 1751–1758.
Duncanson, L., Niemann, K., Wulder, M., 2010. Integration of GLAS and Landsat TM data for aboveground biomass estimation. Can. J. Remote Sens. 36, 129–141.
Dyrness, C.T., 2005. Soil Survey (1964, revised in 1994), Andrews Experimental Forest. Long-Term Ecological Research. Forest Science Data Bank, Corvallis, OR. <http://andrewsforest.oregonstate.edu/data/abstract.cfm?dbcode=SP026&topnav=97> (accessed August 21, 2015).
Fahey, R., Fotis, A.T., Woods, K.D., 2015. Quantifying canopy complexity and effects on productivity and resilience in late successional hemlock-hardwood forests. Ecol. Appl. 25, 834–847.
Food and Agriculture Organization [FAO], 2011. Mountain forests in a changing world – realizing values, addressing challenges. In: Price, M.F., Gratzer, G., Duguma, L.A., Kohler, T., Maselli, D., Romeo, R. (Eds.), Published by FAO/MPS and SDC, Rome.
Franklin, J.F., Spies, T.A., Pelt, R.V., Carey, A.B., Thornburgh, D.A., Berg, D.R., Lindenmayer, D.B., Harmon, M.E., Keeton, W.S., Shaw, D.C., 2002. Disturbances and structural development of natural forest ecosystems with silvicultural implications, using Douglas-fir forests as an example. For. Ecol. Manage. 155, 399–423.
Goodale, C.L., Apps, M.J., Birdsey, R.A., Field, C.B., Heath, L.S., Houghton, R.A., Jenkins, J.C., Kohlmaier, G.H., Kurz, W., Liu, S., 2002. Forest carbon sinks in the northern hemisphere. Ecol. Appl. 12, 891–899.
Gray, A.N., Whittier, T.R., 2014. Carbon stocks and changes on Pacific Northwest national forests and the role of disturbance, management, and growth. For. Ecol. Manage. 328, 167–178.
Griffiths, R.P., Madritch, M.D., Swanson, A.K., 2009. The effects of topography on forest soil characteristics in the Oregon Cascade Mountains (USA): implications for the effects of climate change on soil properties. For. Ecol. Manage. 257, 1–7.
Haining, R., 1993. Spatial Data Analysis in the Social and Environmental Sciences. Cambridge University Press.
Hardiman, B.S., Bohrer, G., Gough, C.M., Vogel, C.S., Curtis, P.S., 2011. The role of canopy structural complexity in wood net primary production of a maturing northern deciduous forest. Ecology 92, 1818–1827.
Harmon, M., Munger, T., 2005. Tree Growth and Mortality Measurements in Long-term Permanent Vegetation Plots in the Pacific Northwest (LTER Reference Stands). Long-term Ecological Research. Forest Science Data Bank, Corvallis, OR. <http://andrewsforest.oregonstate.edu/data/abstract.cfm?dbcode=TV010&topnav=97> (accessed August 21, 2015).
Heyerdahl, E.K., Brubaker, L.B., Agee, J.K., 2001. Spatial controls of historical fire regimes: a multiscale example from the interior west, USA. Ecology 82, 660–678.
Houghton, R., Hackler, J., Lawrence, K., 1999. The US carbon budget: contributions from land-use change. Science 285, 574–578.
Hudak, A.T., Crookston, N.L., Evans, J.S., Hall, D.E., Falkowski, M.J., 2008. Nearest neighbor imputation of species-level, plot-scale forest structure attributes from LiDAR data. Remote Sens. Environ. 112, 2232–2245.
Hudiburg, T., Law, B., Turner, D.P., Campbell, J., Donato, D., Duane, M., 2009. Carbon dynamics of Oregon and Northern California forests and potential land-based carbon storage. Ecol. Appl. 19, 163–180.
Jenkins, J.C., Chojnacky, D.C., Heath, L.S., Birdsey, R.A., 2004. Comprehensive Database of Diameter-based Biomass Regressions for North American Tree Species.
Kane, V.R., McGaughey, R.J., Bakker, J.D., Gersonde, R.F., Lutz, J.A., Franklin, J.F., 2010. Comparisons between field-and LiDAR-based measures of stand structural complexity. Can. J. For. Res. 40, 761–773.
Kashian, D.M., Romme, W.H., Tinker, D.B., Turner, M.G., Ryan, M.G., 2006. Carbon storage on landscapes with stand-replacing fires. Bioscience 56, 598–606.
Keith, H., Mackey, B.G., Lindenmayer, D.B., 2009. Re-evaluation of forest biomass carbon stocks and lessons from the world's most carbon-dense forests. Proc. Natl. Acad. Sci. 106, 11635–11640.
Kindermann, G.E., Schörghuber, S., Linkosalo, T., Sanchez, A., Rammer, W., Seidl, R., Lexer, M.J., 2013. Potential stocks and increments of woody biomass in the European Union under different management and climate scenarios. Carbon Balance Manage. 8.
Kissling, W.D., Carl, G., 2008. Spatial autocorrelation and the selection of simultaneous autoregressive models. Glob. Ecol. Biogeogr. 17, 59–71.
Klinka, K., Carter, R., 1990. Relationships between site index and synoptic environmental factors in immature coastal Douglas-fir stands. For. Sci. 36, 815–830.
Kramer, M.G., Hansen, A.J., Taper, M.L., Kissinger, E.J., 2001. Abiotic controls on long-term windthrow disturbance and temperate rain forest dynamics in southeast Alaska. Ecology 82, 2749–2768.
Kurz, W.A., Dymond, C.C., Stinson, G., Rampley, G.J., Neilson, E.T., Carroll, A.L., Ebata, T., Safranyik, L., 2008. Mountain pine beetle and forest carbon feedback to climate change. Nature 452, 987–990.
Larson, A.J., Lutz, J.A., Gersonde, R.F., Franklin, J.F., Hietpas, F.F., 2008. Potential site productivity influences the rate of forest structural development. Ecol. Appl. 18, 899–910.
Latta, G., Temesgen, H., Barrett, T.M., 2009. Mapping and imputing potential productivity of Pacific Northwest forests using climate variables. Can. J. For. Res. 39, 1197–1207.
Law, B.E., Turner, D., Campbell, J., Sun, O.J., Van Tuyl, S., Ritts, W.D., Cohen, W.B., 2004. Disturbance and climate effects on carbon stocks and fluxes across Western Oregon USA. Glob. Change Biol. 10, 1429–1444.
Lefsky, M.A., Cohen, W.B., Harding, D.J., Parker, G.G., Acker, S.A., Gower, S.T., 2002a. Lidar remote sensing of above-ground biomass in three biomes. Glob. Ecol. Biogeogr. 11, 393–399.
Lefsky, M.A., Cohen, W.B., Parker, G.G., Harding, D.J., 2002b. Lidar remote sensing for ecosystem studies: Lidar, an emerging remote sensing technology that directly measures the three-dimensional distribution of plant canopies, can accurately estimate vegetation structural attributes and should be of particular interest to forest, landscape, and global ecologists. Bioscience 52, 19–30.
Li, Y., Andersen, H.-E., McGaughey, R., 2008. A comparison of statistical methods for estimating forest biomass from light detection and ranging data. West. J. Appl. For. 23, 223–231.
Liaw, A., Wiener, M., 2002. Classification and regression by randomForest. R News 2, 18–22.
Lienkaemper, G., 2004. Managed Stands—Harvest Year. Original GIS Data Catalog for Andrews Experimental Forest. <http://www.andrewsforest.oregonstate.edu/data/spatial/gislist.cfm?-topnav=91> (accessed October 05, 2011).
Lookingbill, T.R., Urban, D.L., 2003. Spatial estimation of air temperature differences for landscape-scale studies in montane environments. Agric. For. Meteorol. 114, 141–151.
Lu, D., 2006. The potential and challenge of remote sensing-based biomass estimation. Int. J. Remote Sens. 27, 1297–1328.
Lundquist, J.D., Cayan, D.R., 2007. Surface temperature patterns in complex terrain: daily variations and long-term change in the central Sierra Nevada, California. J. Geophys. Res.: Atmos. (1984–2012), 112.
Lutz, J.A., Halpern, C.B., 2006. Tree mortality during early forest development: a long-term study of rates, causes, and consequences. Ecol. Monogr. 76, 257–275.
McCardle, R.E., Meyer, W.H., 1930. The yield of Douglas-fir in the Pacific Northwest. US Dept. Agric. Tech. Bull. 201, G4.
McGaughey, R., 2013. FUSION/LDV: Software for LIDAR Data Analysis and Visualization. US Department of Agriculture, Forest Service, Pacific Northwest Research Station, Seattle, WA, USA, p. 123.
Means, J.E., Hansen, H.A., Koerper, G.J., Alaback, P.B., Klopsch, M.W., 1994. Software for Computing Plant Biomass—BIOPAK Users Guide.
Meyer, M.D., North, M.P., Gray, A.N., Zald, H.S., 2007. Influence of soil thickness on stand characteristics in a Sierra Nevada mixed-conifer forest. Plant Soil 294, 113–123.
Morrison, P.H., Swanson, F.J., 1990. Fire History and Pattern in a Cascade Range Landscape. US Dept. of Agriculture, Forest Service, Pacific Northwest Research Station, Portland, OR.
Munger, T.T., 1930. Ecological aspects of the transition from old forests to new. Science 72, 327–332.
Nabuurs, G.-J., Thürig, E., Heidema, N., Armolaitis, K., Biber, P., Cienciala, E., Kaufmann, E., Mäkipää, R., Nilsen, P., Petritsch, R., 2008. Hotspots of the European forests carbon cycle. For. Ecol. Manage. 256, 194–200.
Nelder, J.A., Mead, R., 1965. A simplex method for function minimization. Comput. J. 7, 308–313.
Nemani, R.R., Keeling, C.D., Hashimoto, H., Jolly, W.M., Piper, S.C., Tucker, C.J., Myneni, R.B., Running, S.W., 2003. Climate-driven increases in global terrestrial net primary production from 1982 to 1999. Science 300, 1560–1563.
Oren, R., Ellsworth, D.S., Johnsen, K.H., Phillips, N., Ewers, B.E., Maier, C., Schäfer, K. V., McCarthy, H., Hendrey, G., McNulty, S.G., 2001. Soil fertility limits carbon sequestration by forest ecosystems in a CO_2-enriched atmosphere. Nature 411, 469–472.
Pan, Y., Birdsey, R.A., Fang, J., Houghton, R., Kauppi, P.E., Kurz, W.A., Phillips, O.L., Shvidenko, A., Lewis, S.L., Canadell, J.G., 2011. A large and persistent carbon sink in the world's forests. Science 333, 988–993.
Parker, G.G., Harmon, M.E., Lefsky, M.A., Chen, J., Van Pelt, R., Weis, S.B., Thomas, S. C., Winner, W.E., Shaw, D.C., Frankling, J.F., 2004. Three-dimensional structure of an old-growth Pseudotsuga-Tsuga canopy and its implications for radiation balance, microclimate, and gas exchange. Ecosystems 7, 440–453.
Pelletier, J.D., Rasmussen, C., 2009. Geomorphically based predictive mapping of soil thickness in upland watersheds. Water Resour. Res. 45, W09417.
Perry, D.A., Hessburg, P.F., Skinner, C.N., Spies, T.A., Stephens, S.L., Taylor, A.H., Franklin, J.F., McComb, B., Riegel, G., 2011. The ecology of mixed severity fire regimes in Washington, Oregon, and Northern California. For. Ecol. Manage. 262, 703–717.
Prasad, A.M., Iverson, L.R., Liaw, A., 2006. Newer classification and regression tree techniques: bagging and random forests for ecological prediction. Ecosystems 9, 181–199.
Pregitzer, K.S., Euskirchen, E.S., 2004. Carbon cycling and storage in world forests: biome patterns related to forest age. Glob. Change Biol. 10, 2052–2077.
Pretzsch, H., Biber, P., Schütze, G., Uhl, E., Rötzer, T., 2014. Forest stand growth dynamics in Central Europe have accelerated since 1870. Nat. Commun. 5.
Prichard, S.J., Kennedy, M.C., 2013. Fuel treatments and landform modify landscape patterns of burn severity in an extreme fire event. Ecol. Appl. 24, 571–590.
Pyles, M.R., Mills, K., Saunders, G., 1987. Mechanics and stability of the Lookout Creek earth flow. Bull. Assoc. Eng. Geol. 24, 267–280.
Quine, C.P., White, I.M.S., 1998. The potential of distance-limited topex in the prediction of site windiness. Forestry 71, 325–332.

R Development Core Team, 2012. R: A Language and Environment for Statistical Computing. R Foundation for Statistical Computing, Vienna, Austria.
Ribeiro Jr., P.J., Diggle, P.J., 2001. GeoR: a package for geostatistical analysis. R News 1, 14–18.
Ruel, J.C., Mitchell, S.J., Dornier, M., 2002. A GIS based approach to map wind exposure for windthrow hazard rating. Northern Journal of Applied Forestry 19, 183–187.
Seidl, R., Eastaugh, C.S., Kramer, K., Maroschek, M., Reyer, C., Socha, J., Vacchiano, G., Zlatanov, T., Hasenauer, H., 2013. Scaling issues in forest ecosystem management and how to address them with models. Eur. J. For. Res. 132, 653–666.
Seidl, R., Rammer, W., Spies, T.A., 2014a. Disturbance legacies increase the resilience of forest ecosystem structure, composition, and functioning. Ecol. Appl. 24, 2063–2077.
Seidl, R., Schelhaas, M.-J., Rammer, W., Verkerk, P.J., 2014b. Increasing forest disturbances in Europe and their impact on carbon storage. Nat. Clim. Change 4, 806–810.
Seidl, R., Spies, T.A., Rammer, W., Steel, E.A., Pabst, R.J., Olsen, K., 2012. Multi-scale drivers of spatial variation in old-growth forest carbon density disentangled with Lidar and an individual-based landscape model. Ecosystems 15, 1321–1335.
Sinton, D.S., Jones, J.A., Ohmann, J.L., Swanson, F.J., 2000. Windthrow disturbance, forest composition, and structure in the Bull Run basin, Oregon. Ecology 81, 2539–2556.
Smithwick, E.A.H., Harmon, M.E., Remillard, S.M., Acker, S.A., Franklin, J.F., 2002. Potential upper bounds of carbon stores in forests of the Pacific Northwest. Ecol. Appl. 12, 1303–1317.
Spies, T.A., Franklin, J.F., 1988. Old growth and forest dynamics in the Douglas-fir region of western Oregon and Washington. Nat. Areas J. 8, 190–201.
Spies, T.A., Franklin, J.F., Klopsch, M., 1990. Canopy gaps in Douglas-fir forests of the Cascade Mountains. Can. J. For. Res. 20, 649–658.
Spies, T.A., Franklin, J.F., Thomas, T.B., 1988. Coarse woody debris in Douglas-fir forests of western Oregon and Washington. Ecology 69, 1689–1702.
Swanson, F.J., James, M.E., 1975. Geomorphic history of the lower Blue River-Lookout Creek area, Western Cascades, Oregon. Northwest Sci. 49, 1–11.
Swanson, F.J., Jones, J., 2002. Geomorphology and hydrology of the H.J. Andrews Experimental Forest, Blue River, Oregon. In: Moore, G.W. (Ed.), 98th Annual Meeting of the Cordilleran Section of the Geological Society of America. Oregon Department of Geology and Mineral Industries, Corvallis, Oregon, pp. 288–314.
Swanson, F.J., Swanston, D.N., 1977. Complex mass-movement terrains in the western Cascade Range, Oregon. Rev. Eng. Geol. 3, 113–124.
Taylor, A.H., Skinner, C.N., 2003. Spatial patterns and controls on historical fire regimes and forest structure in the Klamath Mountains. Ecol. Appl. 13, 704–719.
Teensma, P.D.A., 1987. Fire History and Fire Regimes of the Central Western Cascades of Oregon. University of Oregon.
Temesgen, H., Affleck, D., Poudel, K., Gray, A., Sessions, J., 2015. A review of the challenges and opportunities in estimating above ground forest biomass using tree-level models. Scand. J. For. Res. 30, 326–335.
Tepley, A.J., 2010. Age Structure, Developmental Pathways, and Fire Regime Characterization of Douglas-fir/Western Hemlock Forests in the Central Western Cascades of Oregon. PhD Dissertation, Oregon State University, Corvallis, OR.
Tepley, A.J., Swanson, F.J., Spies, T.A., 2013. Fire-mediated pathways of stand development in Douglas-fir/western hemlock forests of the Pacific Northwest, USA. Ecology 94, 1729–1743.
Thompson, J.R., Spies, T.A., Ganio, L.M., 2007. Reburn severity in managed and unmanaged vegetation in a large wildfire. Proc. Natl. Acad. Sci. 104, 10743–10748.
Tromp-van Meerveld, H.J., McDonnell, J.J., 2006. On the interrelations between topography, soil depth, soil moisture, transpiration rates and species distribution at the hillslope scale. Adv. Water Resour. 29, 293–310.
Turner, D.P., Cohen, W.B., Kennedy, R.E., Fassnacht, K.S., Briggs, J.M., 1999. Relationships between leaf area index and landsat TM spectral vegetation indices across three temperate zone sites. Remote Sens. Environ. 70, 52–68.
Turner, D.P., Ritts, W.D., Cohen, W.B., Gower, S.T., Zhao, M., Running, S.W., Wofsy, S. C., Urbanski, S., Dunn, A.L., Munger, J.W., 2003. Scaling Gross Primary Production (GPP) over boreal and deciduous forest landscapes in support of MODIS GPP product validation. Remote Sens. Environ. 88, 256–270.
UNFCCC, 2009. Fifteenth Session of the Conference of Parties to the United Nations Framework Convention on Climate Change. Copenhagen Accord. <http://unfccc.int/documentation/documents/advanced_search/items/3594.php?rec=j&priref=6000 05735#beg> (last accessed January 16, 2016).
Urban, D., Miller, C., Halpin, P., Stephenson, N., 2000. Forest gradient response in Sierran landscapes: the physical template. Landscape Ecol. 15, 603–620.
U.S. Environmental Protection Agency [EPA], 2015. Inventory of U.S. Greenhouse Gas Emissions and Sinks: 1990–2013. 430-R-15-004. <http://www.epa.gov/climatechange/Downloads/ghgemissions/US-GHG-Inventory-2015-Main-Text.pdf> (last accessed January 16, 2016).
Van Tuyl, S., Law, B., Turner, D., Gitelman, A., 2005. Variability in net primary production and carbon storage in biomass across Oregon forests—an assessment integrating data from forest inventories, intensive sites, and remote sensing. For. Ecol. Manage. 209, 273–291.
Ver Hoef, J.M., Temesgen, H., 2013. A comparison of the spatial linear model to nearest neighbor (k-NN) methods for forestry applications. PloS one 8.3, e59129.
Weisberg, P.J., 1998. Fire history, fire regimes, and development of forest structure in the central western Oregon Cascades. PhD Dissertation. Oregon State University, Corvallis, OR.
Weisberg, P.J., Swanson, F.J., 2003. Regional synchroneity in fire regimes of western Oregon and Washington, USA. For. Ecol. Manage. 172, 17–28.
Weisberg, P.J., 2004. Importance of non-stand-replacing fire for development of forest structure in the Pacific Northwest, USA. For. Sci. 50, 245–258.
Whittaker, R., Bormann, F., Likens, G., Siccama, T., 1974. The Hubbard Brook ecosystem study: forest biomass and production. Ecol. Monogr. 44, 233–254.
Whittaker, R.H., 1966. Forest dimensions and production in the Great Smoky Mountains. Ecology, 103–121.
Whittaker, R.H., 1978. Ordination of Plant Communities. W. Junk The Hague.
Whittaker, R.H., Niering, W.A., 1975. Vegetation of the Santa Catalina Mountains, Arizona. V. Biomass, production, and diversity along the elevation gradient. Ecology, 771–790.
Wimberly, M.C., Cochrane, M.A., Baer, A.D., Pabst, K., 2009. Assessing fuel treatment effectiveness using satellite imagery and spatial statistics. Ecol. Appl. 19, 1377–1384.
Woodbury, P.B., Smith, J.E., Heath, L.S., 2007. Carbon sequestration in the US forest sector from 1990 to 2010. For. Ecol. Manage. 241, 14–27.
Zald, H.S., Ohmann, J.L., Roberts, H.M., Gregory, M.J., Henderson, E.B., McGaughey, R. J., Braaten, J., 2014. Influence of lidar, Landsat imagery, disturbance history, plot location accuracy, and plot size on accuracy of imputation maps of forest composition and structure. Remote Sens. Environ. 143, 26–38.